COD Removal from Artificial Wastewater by Electrocoagulation Using Aluminum Electrodes

Q.H. Nguyen[1], T. Watari[2], T. Yamaguchi[2,3], Y. Takimoto[3], K. Niihara[1], J.P. Wiff[3] and T. Nakayama[1*].

[1] Extreme Energy-Density Research Institute, Nagaoka University of Technology, 1603-1 Kamitomioka, Nagaoka, Niigata, 940-2188, Japan
[2] Department of Civil and Environmental Engineering, Nagaoka University of Technology, 1603-1 Kamitomioka, Nagaoka, Niigata, 940-2188, Japan
[3] Department of Science of Technology Innovation, Nagaoka University of Technology, 1603-1 Kamitomioka, Nagaoka, Niigata, 940-2188, Japan
[*]E-mail: nky15@vos.nagaokaut.ac.jp

This study investigates the effects of pH, treatment time, distance between electrodes, and voltage on the efficiency of chemical oxygen demand (COD) removal from artificial wastewater through an electrocoagulation (EC) process. Anode and cathode electrodes were fabricated using commercial Al plates. The results demonstrate that the COD removal efficiency can be increased to 51% when the initial pH is 4.1. Moreover, pH had the largest impact on the COD removal efficiency compared to the other parameters. At low initial pH, insoluble compounds were formed, increasing the COD removal efficiency. Whereas at high initial pH, the formation of soluble compounds was favored, resulting in a net reduction of COD removal efficiency. Furthermore, a correlation between the varying sizes of hydrogen bubbles and COD removal efficiency was observed at different pH values. The results suggest that a narrow hydrogen bubble-size distribution of approximately 42 µm can increase the COD removal efficiency because of the enhancement of the flotation mechanism during EC. Finally, the results from X-ray diffraction and energy dispersive spectroscopy suggest that flotation provides better adsorption than precipitation during EC.

1. INTRODUCTION

Chemical oxygen demand (COD) is a traditional and widely used indicator of water quality. COD quantifies the amount of oxygen used for the chemical oxidation of inorganic and organic matter contained in the wastewater. Causes for high COD include biodegradable organic, non-biodegradable, and inorganic oxidizable compounds [1].

Electrocoagulation (EC) is a promising water-treatment process because of its simple design and operation. However, the high cost of electricity is the main barrier impeding its use in industrial

applications [2, 3]. Recently, the incipient promotion of renewable energy sources has decreased energy costs, generating new interest in the EC process for the treatment of industrial wastewater. Moreover, the use of renewable energy sources with EC processing can promote an eco-friendly method of wastewater treatment.

Recently, EC has been used in industrial applications, such as for the treatment of municipal wastewater, textile wastewater, poultry manure wastewater, landfill leachate, rose processing wastewater, chemical mechanical polishing wastewater, etc. [4]. However, several uncertainties and challenges remain regarding the transition from laboratory to industrial scales.

Despite the impressive amount of research on the wastewater treatment using EC, no applications of EC for COD removal from artificial wastewater (based on Organization for Economic Cooperation and Development (OECD) standards) have been investigated. Moreover, during EC, the relationship between pH variations and other parameters (e.g., treatment time and applied voltage) and COD removal efficiency has received inadequate attention. This investigation seeks clarification of this relationship, especially between pH variation and treatment time on COD removal efficiency. In the extant literature, little or no consideration has been paid to the relationship between hydrogen bubble size and COD removal efficiency during EC. Therefore, this study aims to assess this relationship. Furthermore, very few studies have examined the characterization of precipitation and flotation using X-ray diffraction (XRD) and energy dispersive spectroscopy (EDS), after EC with Al electrodes to remove COD from wastewater. In this study, the efficiency of precipitation and flotation on COD removal from artificial wastewater is compared based on EC by-product characterizations.

EC promotes the formation of coagulant species from the electrolytic oxidation of a sacrificial anode triggered by an electric current passing through electrodes. EC significantly reduces the formation of sub-products and sludge during treatment. Moreover, the sludge generated by EC processes tends to be less toxic than those generated by other chemical water purification processes. Furthermore, they are easy to separate via precipitation or flotation using the hydrogen microbubbles formed at the cathode [5].

A typical EC system can use direct current (DC), alternating current (AC), or alternating pulsed current (APC) as the power supply to create an electrochemical cell between the anode and cathode immerged in the wastewater. Metal ions are generated via oxidation at the anode, and hydroxides (OH⁻) are generated by reduction at the cathode. Metal ions and hydroxides combine in the solution, producing metal hydroxides with a high ability for physical adsorption [6, 7]. Thus, coagulant particles can adsorb ions and other micro-colloidal particles from the wastewater for removal by precipitation or flotation.

Usually, Fe and Al are used as electrodes, because they are commercially available at a low cost, and their hydroxides exhibit low toxicity and high valence after precipitation, enhancing their pollutant-removal capability [8]. Nonetheless, Al is preferred, because it is stable, easily handled, and readily soluble [9].

Typical reactions of Al at the anode and cathode can be understood as follows:

At the anode, Al oxidizes to form Al^{3+} cations [8].

$$Al - 3e = Al^{+3} \tag{1}$$

However, at high anodic potential, secondary reactions may occur [10, 11]. For instance, water can oxidize, forming hydronium cation and oxygen gas. However, in the solution, chloride anions can

be oxidized into Cl_2, contributing to the oxidation of dissolved organic compounds or to the formation of ClOH [12].

$$2H_2O - 4e = O_2 + 4H^+ \qquad (2)$$
$$2Cl^- - 2e = Cl_2 \qquad (3)$$
$$Cl_2 + H_2O = ClOH + H^+ + Cl^- \qquad (4)$$
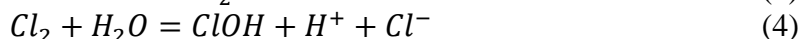
At the cathode, water is reduced into hydrogen gas and hydroxyl anions [8].

$$2(H_2O) + 2e^- = H_2 + 2(OH^-) \qquad (5)$$
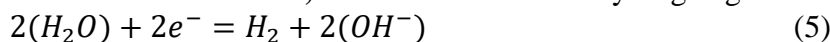
EC is affected by the pH of wastewater, which controls the solubility of products formed during electrolysis. For the Al-based electrodes, the Pourbaix diagram suggests that, at a pH<4, soluble species Al^{+3} ions are the main product of EC, whereas at 4<pH<10, the formation of the insoluble compound $Al(OH)_3$ is favored. At pH>10, the soluble $Al(OH)_4^-$ tends to be formed according to Reaction (6) [8, 13]. Therefore, pH is essential to controlling the product species and their solubility in wastewater.

$$Al + 4OH^- = [Al(OH)_4]^- + 3e \qquad (6)$$

Anode dissolution and combination with OH⁻ groups from the cathode may occur via monomeric and polymeric reactions of Al^{3+} and $Al(OH)_2^+$ species [4]. Additionally, hydrogen bubbles are generated by the reduction process at the cathode, whereas only a few oxygen bubbles are released from the anode [14]. The size of the bubbles can significantly influence their retention time and stability in the solution. Large bubbles tend to rise quickly to the surface, decreasing the possibility of capturing pollutants. In contrast, microbubbles (20 – 50 µm) can increase the retention time by several orders of magnitude [15]. Consequently, this increases the probability of catching pollutants from the solution and enhancing the COD removal efficiency. This study used the Sauter (D_{32}) average diameter to determine the hydrogen bubble sizes (see Equation 7). The correlation between their size and COD removal efficiency, D_{32}, is considered an appropriate flotation metric, because it is defined as the average diameter of volume to surface-area ratio of all bubbles, where active surface area is important [16].

$$D_{32} = \frac{\sum_{i=0}^n d_i^3}{\sum_{i=0}^n d_i^2} \qquad (7)$$

where d_i is the bubble diameter, and n is the number of bubbles obtained from the bubble-size measurement.

2. EXPERIMENTAL

2.1. EC cell

Figure 1 shows the EC setup used in this study. The EC reactor comprised a 300-ml beaker containing 200 ml of a standard artificial wastewater. Anode and cathode electrodes were fabricated by using commercial Al plates. All electrodes were 55×20×1 mm³ each, located as shown in Figure 1. The distance between electrodes (x) was evaluated from 0.5–2.0 cm. A DC power supply (PL-650-0.1, Matsusada Co. Ltd., Japan) was used in potentiostatic mode from 5–18 V during different treatment times. The artificial wastewater was stirred at 200 rpm at room temperature to enhance contact between pollutants and the metal hydroxide adsorbent formed during EC.
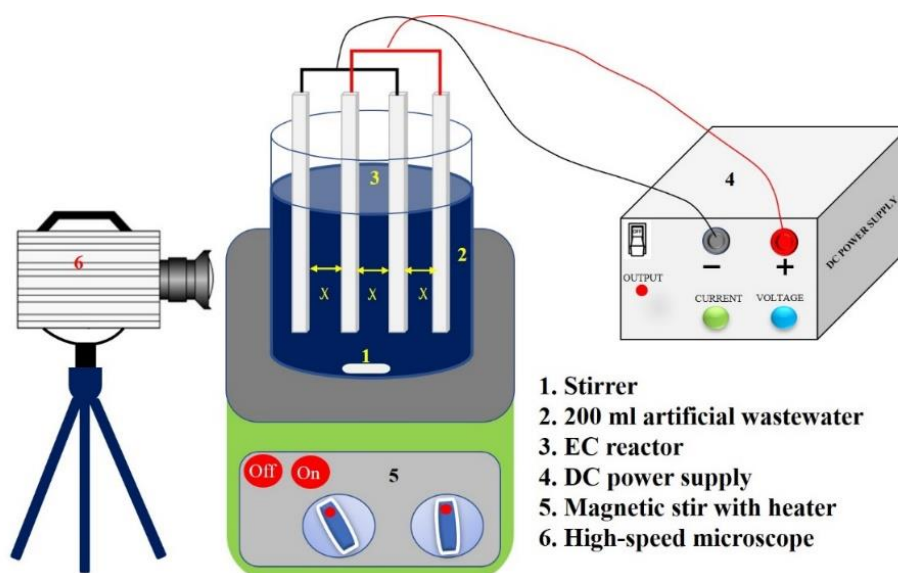
Figure 1. Schematic of laboratory-scale EC reactor at the same separation for all cases (χ = 1 cm)

2.2. Artificial wastewater

Table 1. Composition of the artificial wastewater, OECD standard

Composition	Peptone	Meat extract	Urea	NaCl	CaCl$_2$	MgSO$_4$	K$_2$PO$_4$
Weight (g)	16	11	3	0.7	0.4	0.2	2.8

Table 1 shows the artificial wastewater composition proposed by OECD as a standard solution to evaluate wastewater treatments [17]. The nominal composition was diluted in 1 L of deionized water and stirred for 1 h. Artificial wastewater was stored up to 1 week in a dark room at 4 °C. HCl and NaOH were used to adjust the initial pH of artificial wastewater. Electrical conductivity and pH were recorded immediately after the EC experiments with a pH meter (Model HM-30R, range from 0.000–14) and a COND meter (Model ES-71), respectively. COD was measured using the HACH 8000 method. Each COD measurement was performed in duplicate or triplicate to ensure the repeatability of results.

The COD removal efficiency (η) at time *t* is defined as:

$$\eta(t) = \frac{COD_0 - COD_t}{COD_0} * 100 \tag{8}$$

where COD_0 and COD_t correspond to the COD at the beginning and at time *t* of the experiment, respectively.

The precipitation and flotation characteristics and the anode surface were analyzed using field emission scanning electron microscopy (FE-SEM) (JEOL JSM-6700F), energy dispersive spectroscopy (EDS), and X-ray diffraction (XRD) (Rigaku RINT-2500, CuK).

2.3. Bubble size

The size variation of hydrogen bubbles at the cathode was recorded using a high-speed microscope (Keyence VW-9000m, Japan). Recording parameters were set to: 6,000-s shutter speed, 2,000 fps frame rate, 640×480 resolution, and ×200 magnification. The size and distribution of the bubbles were calculated using ImageJ software [18], examining at least 1,000 bubbles for each experiment.

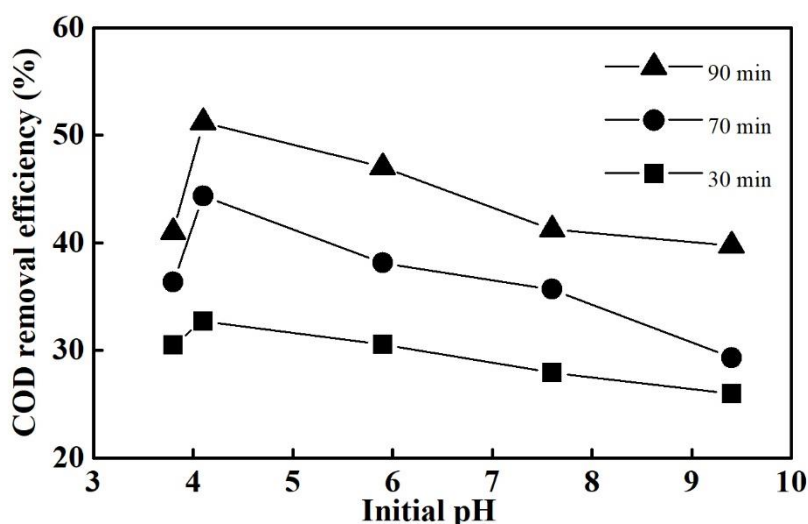## 3. RESULTS AND DISCUSSION

3. 1. Effect of initial pH on COD removal efficiency

Figure 2. Effect of initial pH on the COD removal efficiency for different treatment times under 15 V

Figure 2 shows the COD removal efficiency (η) as a function of the initial pH of artificial wastewater for different treatment times. The maximum COD removal efficiency was 51%, observed at pH = 4.1. This can be attributed to the simultaneous varying formation of monomeric and polymeric species that eventually changed into $Al(OH)_3$, as indicated by the complex precipitation. These $Al(OH)_3$ compounds have large surface areas and act as a coagulant. Thus, they are useful for the fast adsorption of soluble organic compounds and metal ions, resulting in a high COD removal efficiency [19–21]. However, the COD removal efficiency decreased at the initial pH except for 4.1. This may have been caused by the amphoteric characteristic of $Al(OH)_3$, which converted to Al^{3+} and $Al(OH)_4^-$ when the initial pH was low or high, respectively [8, 13]. Generally, the formation of soluble products is predominant at high and very low initial pH, causing COD removal efficiency to gradually decrease.
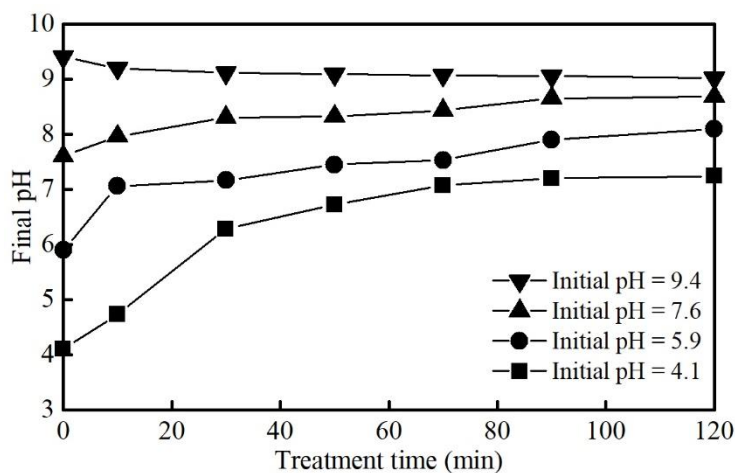
Figure 3. Variation of pH as a function of treatment time at different initial pH under 15 V

Figure 3 shows the variation of pH as a function of treatment time at different initial pH conditions. At an initial pH<9, the final pH increased with treatment time for two reasons: hydrogen evolution at the cathode and partial exchange of Cl^-, SO_4^{2-}, and PO_4^{2-} anions with OH^- in $Al(OH)_3$ to release free OH^- groups [12]. In contrast, at an initial pH>9, both Ca^{2+} and Mg^{2+} cations coprecipitated with $Al(OH)_3$, leading to a net pH decrease. Moreover, at an initial pH>9, the formation of $Al(OH)_4^-$ was predominant, which reduced the final pH of the artificial wastewater [5, 12]. Additionally, Figure 3 shows no significant final pH variation for treatment time of over ~90 min, suggesting that the initial pH determines the long-term operating conditions of the EC process.

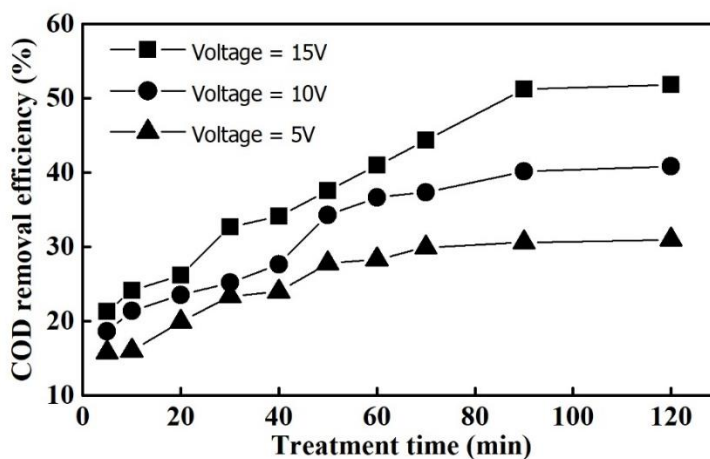*3.2. Effect of treatment time on COD removal efficiency*

Figure 4. Effect of treatment time on COD removal efficiency at pH 4.1

Figure 4 presents the rate of change of COD removal efficiency (η) as a function of treatment time for different voltages. Maximum COD removal efficiency was achieved faster at low voltages than at higher ones. This can be attributed to the fact that low voltages were insufficient to promote the formation of $Al(OH)_3$ compounds, despite the increase in treatment time. On the other hand, regardless of voltages, all experiments reached maximum or saturated COD removal efficiency (η) after 90 min, and the efficiency remained nearly constant afterwards. This trend was in excellent agreement with the

changes of initial pH observed in Figure 3. The pH increased quickly from 10–90 min, suggesting that the amount of hydrogen bubbles increased according to Reaction (5). These bubbles improved the mixing degree of $Al(OH)_3$ and pollutants, which enhanced the flotation ability of the cell and led to an increase in the overall COD removal efficiency [4]. Moreover, COD removal efficiency depends on the quantity of aluminum and hydroxyl ions generated in the solution. When the treatment time increases, the amount of aluminum dissolved in the medium increases, and the production of hydroxyl ions also increase. Consequently, promoting the amount of $Al(OH)_3$ formation causes more pollutants to be adsorbed by $Al(OH)_3$, enhancing COD removal efficiency [22].

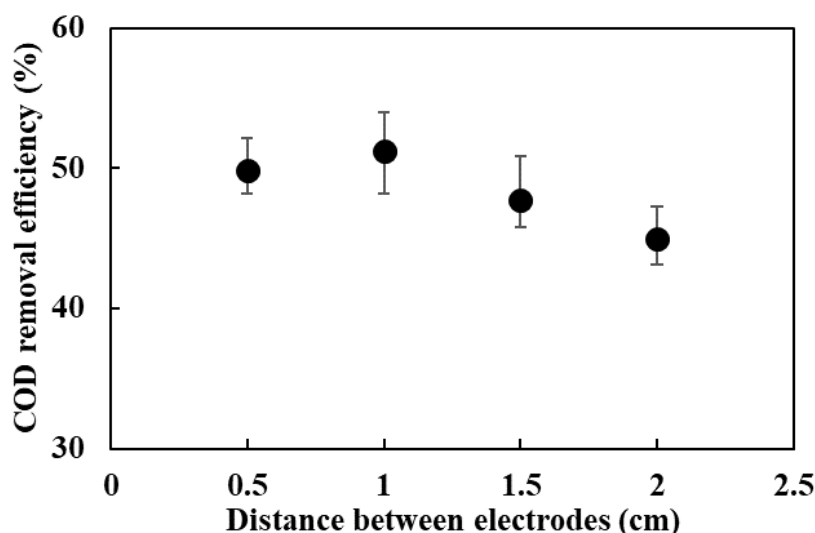*3.3. Effect of the distance between electrodes on COD removal efficiency*

Figure 5. Effect of the distance between electrodes on COD removal efficiency at 15 V, initial pH of 4.1, and treatment time of 90 min

Figure 5 shows the effect of the distance between electrodes (x) on COD removal efficiency. Maximum COD removal efficiency was observed at $x=1$ cm. This result can be explained by the fact that, at short inter-electrode distances, higher electrostatic attraction occurs. Therefore, the generated $Al(OH)_3$ acted as a coagulant and removed pollutants by sedimentation, but the ability was degraded by collisions with each other. However, when the inter-electrode distance increases, the electrostatic effect decreases. Thus, the movement of generated ions is slower, providing more time to form $Al(OH)_3$ compounds for the aggregation and precipitation of suspended particles and for the adsorption of dissolved pollutants. This enhances COD removal efficiency. However, when the distance between electrodes increases above the optimum ($x=1$ cm), the travel times of the ions increase excessively, reducing the formation of flocs needed to coagulate soluble organic compounds and metal ions, resulting in decreased COD removal efficiency [23–25].

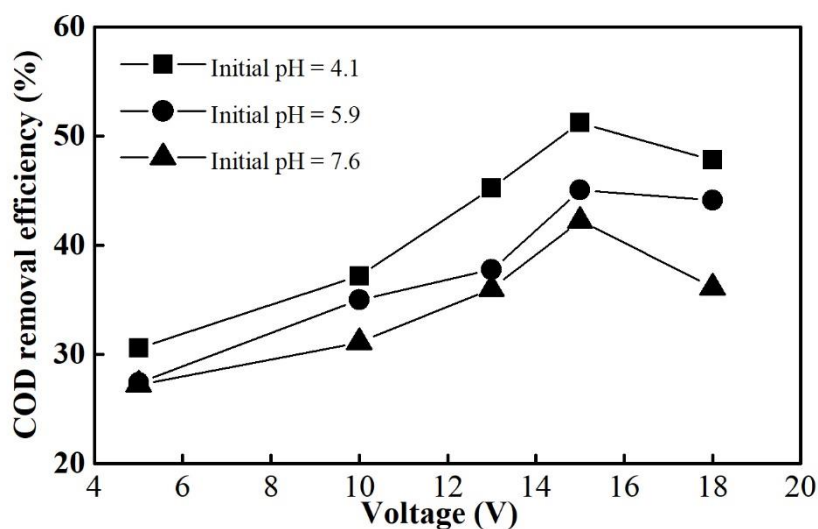*3.4. Effect of applied voltage on COD removal efficiency*

Figure 6. Effect of applied voltage on COD removal efficiency under a 90-min treatment

Figure 6 shows the variation of COD removal efficiency as a function of applied voltage for different initial pH of artificial wastewater. Regardless of initial pH, the COD removal efficiency increased with the application of voltage on the reactor, showing that the maximum COD removal efficiency of 51% occurred at an applied voltage of 15 V. This result agrees with Figure 4, in which COD removal efficiency becomes saturated and approaches its maximum faster at lower voltages. It can be understood that, below the optimum voltage (15 V), soluble Al^+ is predominant in the solution. Hence, the coagulation effects are less significant. Furthermore, when low voltage is applied to the Al anodes that is insufficiently to produce a larger number of Al^{3+} ions, increasing the coagulation capability, and more bubbles are generated from the cathode, enhancing flotation ability. Therefore, COD removal efficiency was low. In contrast, above the optimum voltage, more bubbles are generated from the anode, implying a higher oxygen formation. Therefore, competition between aluminum dissolution and oxygen evolution occurred. Thus, $Al(OH)_3$ formation was reduced, leading to a decrease in COD removal efficiency [14, 26].

3.5. Correlation between hydrogen bubbles size and COD removal efficiency

Figure 7 shows that the Sauter diameter decreased from 45 to 36 µm as the initial pH of artificial wastewater increased from 3.8–9.4. Generally, high pH leads to a reduction in hydrogen bubble size. Therefore, the size depends on the H^+ ion concentration. When the H^+ ion concentration is low, the diameter of the hydrogen bubbles is small and vice versa [27, 28]. The H^+ concentration decreased significantly because of the alkaline wastewater environment, resulting in a smaller volume of nucleated hydrogen bubbles, as shown by the Sauter diameter in Figure 7.
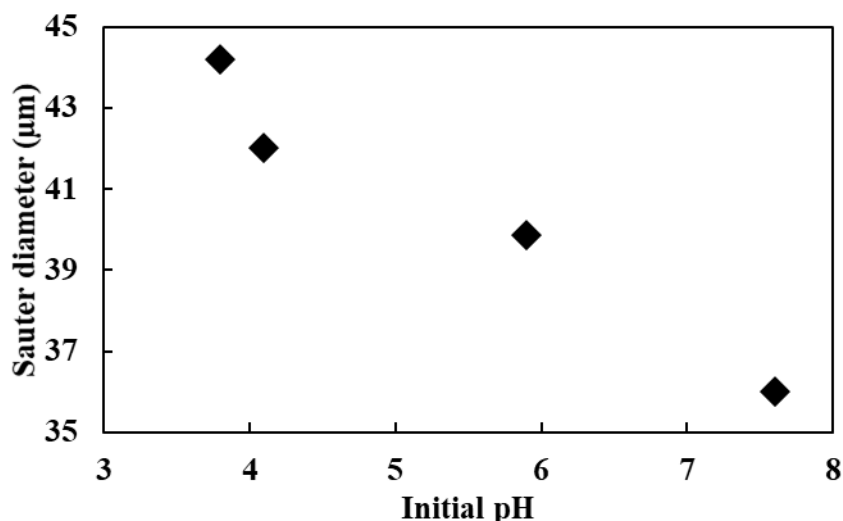
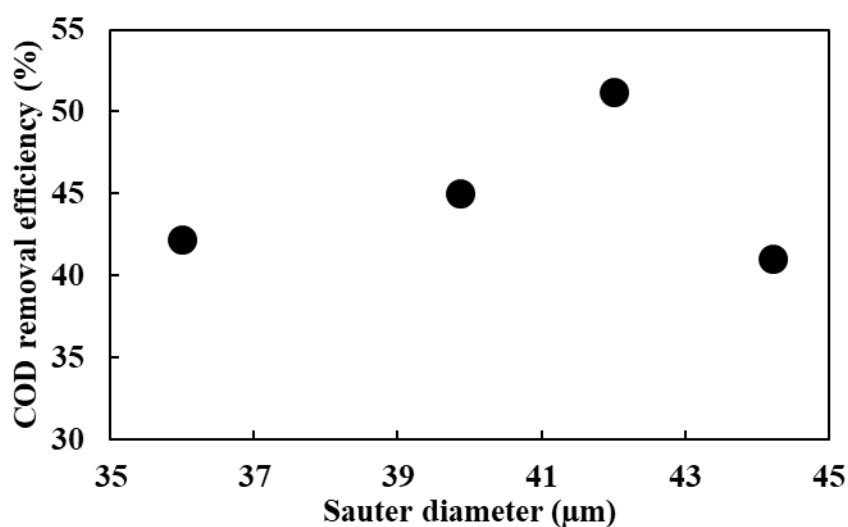**Figure 7.** Sauter diameter as a function of initial pH at 15 V, 90 min

Figure 8. COD removal efficiency as a function of the Sauter diameter at different initial pH, 15 V, and 90-min treatment

Figure 8 shows the COD removal efficiency as a function of the Sauter diameter of hydrogen bubbles. Maximum COD removal efficiency was observed at hydrogen-bubble sizes of ~42 μm. Small hydrogen bubbles are easily dragged around by the fluid movement, restricting their ascent and promoting foamy formations. In contrast, large bubbles sizes easily collapse during their rise, decreasing the contribution of flotation to the reduction of COD removal. Thus, these study results imply that hydrogen bubble sizes of ~42 μm promote flotation, which contributes to pollutant removal from media, resulting in increased COD removal efficiency. Therefore, the results suggest that a proper method to identify the net contribution of the flotation mechanism to COD removal efficiency should include control of the initial and final pH during the EC and controlled hydrogen bubble size, which governs flotation efficiency. This could be accomplished by using an external bubble generator.

3.6. SEM, XRD, and EDS analysis

Figure 9 shows the morphology of the anode surface before (Figure 9a) and after (Figure 9b) the EC process. The results reveal that the surface of the anode was rough and that indentations were established. This was caused by Al dissolution after EC. The formation of indentations can be attributed to the consumption of anode material at the active sites due to the production of oxygen at the surface [29].
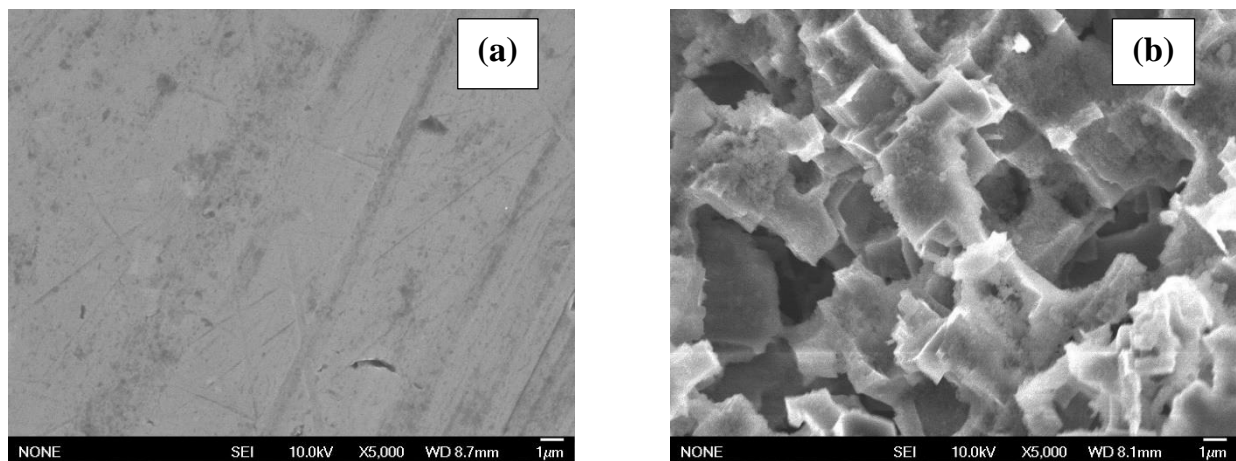

Figure 9. SEM image of anode electrode (a) before and (b) after the EC process
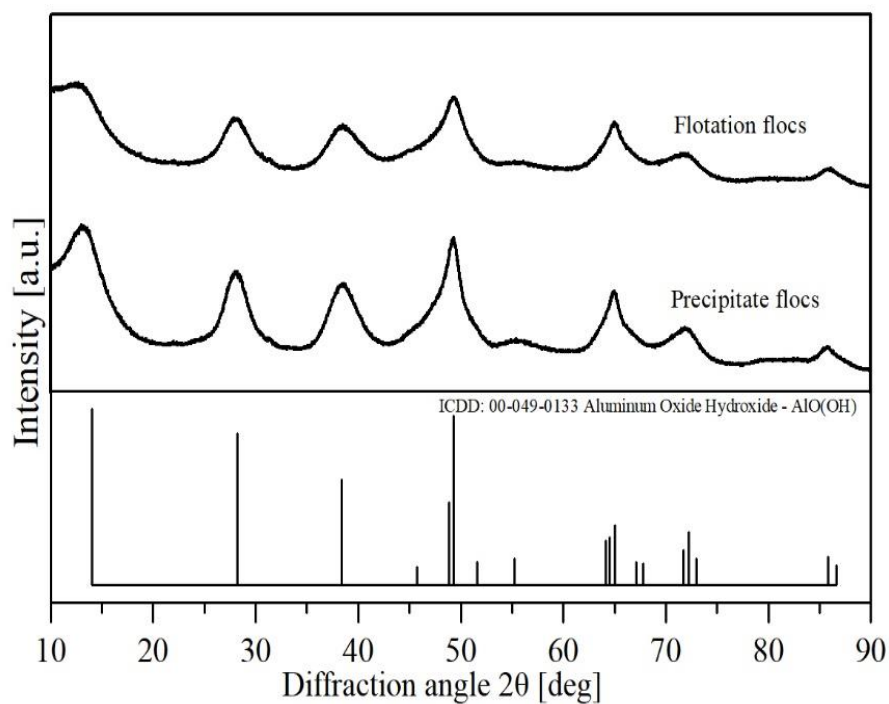

Figure 10. XRD patterns of flotation and precipitation of EC-generated sludge

Figure 10 shows the XRD pattern of flotation and precipitation after the EC process. The signal intensities from the XRD diffraction of flotation were slightly lower than that of precipitation. The decrease of intensity can be attributed to better soluble organic compound adsorption during flotation [30]. Moreover, XRD signals were found to match the values of aluminum oxide hydroxide in both flotation and precipitation (ICDD 00-049-0133). The diffraction signal of the other elements was absent because of the low content in crystallites, such that the signal was covered by that of hydroxides.
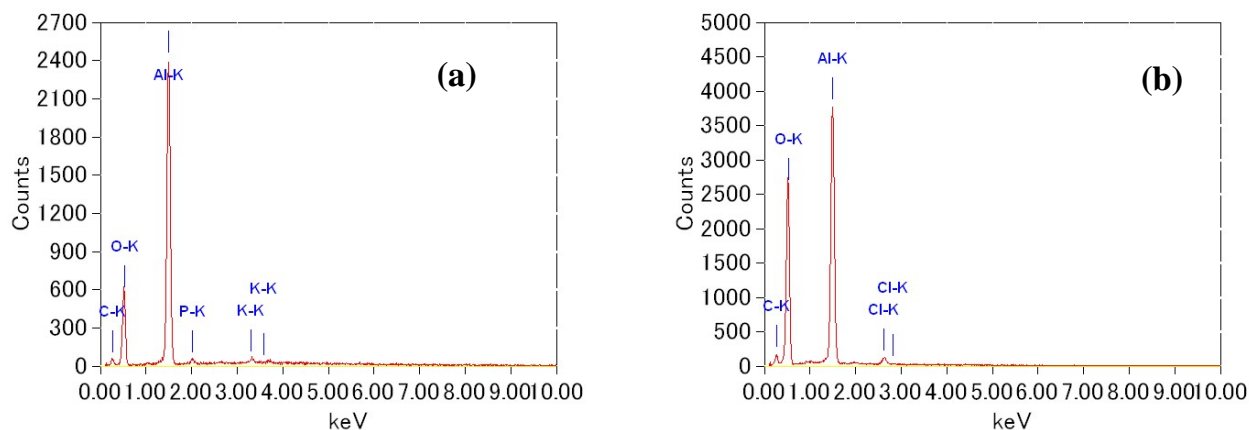

Figure 11. Characterization of the by-products from EC: (a) flotation and (b) precipitation

Figure 11 shows that the by-products formed during EC were composed of elements, such as Al, O, P, K, and Cl. This analysis confirmed that C, P, and K were entrapped within the $Al(OH)_3$ complex and were removed by flotation (Figure 11a). However, Cl was adsorbed by the coagulant and formed a sludge that was removed via precipitation (Figure 11b). The results from Figs. 10 and 11 suggest that flotation can adsorb more pollutants than precipitation. Therefore, a bubble generator and pH control could enhance the flotation function, thus increasing COD removal efficiency.

4. CONCLUSIONS

EC was used to reduce the COD from artificial wastewater. The highest COD removal efficiency (51%) was achieved by using commercial Al plates as anodes and cathodes and by setting the initial pH to 4.1. The initial pH seems to control the variation of pH in the effluent during EC, consequently determining the final COD removal efficiency of the wastewater treatment. Thus, with an initial pH of 4.1, the main EC products were insoluble $Al(OH)_3$. Whereas at a higher initial pH, a gradual formation of soluble Al^{3+}-based species was promoted and, thus, the final COD removal efficiency presented a lower yield. Moreover, a minimum voltage (15 V) can be applied to promote an adequate formation rate of insoluble species from anode dissolution and cathode hydrogen bubbling. Additionally, hydrogen bubble size contributed to COD removal efficiency by controlling the yield of the flotation process. Hydrogen bubble sizes of ~42 µm was preferred to enhance the flotation process. Nevertheless, further experiments should be performed to determine the impact of the flotation mechanism on the wastewater purification process under EC. For example, this could be accomplished by using external bubble

generators and controlling the initial and final pH. Finally, the results showed that flotation was better than precipitation in removing pollutants from wastewater.

References

1. H. A. Moreno-Casillas, D. L. Cocke, J. A. G. Gomes, P. Morkovsky, J. R. Parga and E. Peterson, *Sep. Purif. Technol.*, 56 (2007) 204.
2. M. Y. Mollah, P. Morkovsky, J. A. Gomes, M. Kesmez, J. Parga and D. L. Cocke, *J. Hazard. Mater.,* 114 (2004) 199.
3. M. Y. A. Mollah, R. Schennach, J. R. Parga and D. L. Cocke, *J. Hazard. Mater.*, 84 (2001) 29.
4. B.-y. Tak, B.-s. Tak, Y.-j. Kim, Y. J. Park, Y.-h. Yoon and G.-h. Min, *J. Ind. Eng. Chem.*, 28 (2015) 307.
5. W. Balla, A. H. Essadki, B. Gourich, A. Dassaa, H. Chenik and M. Azzi, *J. Hazard. Mater.*, 184 (2010) 710.
6. J. Lu, Z. Wang, X. Ma, Q. Tang and Y. Li, *Chem. Eng. Sci.,* 165 (2017) 165.
7. M. A. Abdel-Fatah, A. M. Awad, E. M. Ahmed and A. T. El-Aref, *Int. J. Sci. Eng. Res.,* 6 (2015) 1133.
8. J. N. Hakizimana, B. Gourich, M. Chafi, Y. Stiriba, C. Vial, P. Drogui and J. Naja, *Desalination*, 404 (2017) 1.
9. M. Vepsäläinen, Electrocoagulation in the treatment of industrial waters and wastewaters, VTT Technical Research Centre of Finland, 2012.
10. A. Vlyssides, P. Karlis and A. Zorpas, *Environ. Int.*, 25 (1999) 663.
11. G. Mouedhen, M. Feki, M. De Petris Wery and H. F. Ayedi, *J. Hazard. Mater.*, 150 (2008) 124.
12. X. Chen, G. Chen and P. L. Yue, *Sep. Purif. Technol.*, 19 (2000) 65.
13. D. T. Moussa, M. H. El-Naas, M. Nasser and M. J. Al-Marri, *J. Environ. Manage.*, 186 (2017) 24.
14. I. Heidmann and W. Calmano, *J. Hazard. Mater.*, 152 (2008) 934.
15. G. Bhaskar Raju and P. R. Khangaonkar, *Trans Indian Inst Metals.*, 37 (1984) 59.
16. B. A. Wills and J. A. Finch, Wills' mineral processing technology: an introduction to the practical aspects of ore treatment and mineral recovery, Butterworth–Heinemann, (2015) Oxford, United Kingdom.
17. OECD, OECD Guidelines for the testing of chemicals, September 2009/JA.
18. M. D. Abràmoff, P. J. Magalhães and S. J. Ram, *Biophotonics Int.*, 11 (2004) 36.
19. H. Inan, A. Dimoglo, H. Şimşek and M. Karpuzcu, *Sep. Purif. Technol.*, 36 (2004) 23.
20. M. Kobya, C. Ciftci, M. Bayramoglu and M. T. Sensoy, *Sep. Purif. Technol.*, 60 (2008) 285.
21. M. Kobya, O. T. Can and M. Bayramoglu, *J. Hazard. Mater.*, 100 (2003) 163.
22. Z. Zaroual, H. Chaair, A. H. Essadki, K. El Ass and M. Azzi, *Chem. Eng. J.,* 148 (2009) 488.
23. A. A. Bukhari, *Bioresour. Technol.*, 99 (2008) 914.
24. S. Aoudj, A. Khelifa, N. Drouiche, R. Belkada and D. Miroud, *Chem. Eng. J.,* 267 (2015) 153.
25. S. K. Verma, V. Khandegar and A. K. Saroha, *J. Hazard. Toxic Radioact. Waste,* 17 (2013) 146.
26. P. Cañizares, M. Carmona, J. Lobato, F. Martínez and M. A. Rodrigo, *Ind. Eng. Chem. Res.*, 44 (2005) 4178.
27. S. G. da Cruz, A. J. B. Dutra and M. B. M. Monte, *J. Environ. Chem. Eng.*, 4 (2016) 3681.
28. R. R. Hacha, M. LeonardoTorem, A. Gutiérrez Merma and V. F. da Silva Coelho, *Miner. Eng.,* 126 (2018) 105.

29. S. Vasudevan, B. S. Kannan, J. Lakshmi, S. Mohanraj and G. Sozhan, *J. Chem. Technol. Biotechnol.,* 86 (2011) 428.
30. K. Govindan, Y. Oren and M. Noel, *Sep. Purif. Technol.,* 133 (2014) 396.